Chempublish Journal
Journal Homepage: online-journal.unja.ac.id/chp
Department of Chemistry
Faculty of Science and Technology
Universitas Jambi
ISSN (Online): ISSN 2503-4588
No. 23/E/KPT/2019

Article

Synthesis and Characterization of Alginate/PVA/Fe_3O_4 as an Adsorbent for p-Nitrophenol Adsorption

Sonya Nurizki Vikandari*; Fina Ahmad Fitriana, Nia Setiawati, Negi Rahmah Azizia

Department of Pharmacy, Faculty of Health Science, Universitas Perjuangan Tasikmalaya, Tasikmalaya 46115, West Java, Indonesia

Abstract

p-nitrophenol (PNP) is one of the priority pollutants in the environment because i tis toxic properties and a persistent organic pollutant (POP), so it requires greater attention in waste treatment to maintain human health and aquatic ecosystems. Adsorption is one of the pollutant removal methods that has the advantage of being simple and low-cost. This study aims to synthesis and characterize an alginate/polyvinyl alcohol (PVA)/Fe_3O_4 adsorbent and evaluate its performance for PNP removal from aqueous solutions. Alginate is one of the biosorbents that can be used to adsorb liquid waste, but it has weak mechanical properties, so it can be modified with PVA to form a beads adsorbent. The addition of magnetic Fe_3O_4 to the adsorbent aims to provide magnetic properties to facilitate the separation of the adsorbent from the analyte. The adsorbent has been characterized using Fourier Transform Infra Red Spectroscopy (FTIR), Scanning Electron Microscopy (SEM), X-Ray Diffraction (XRD), and Delsa™ Nano C Particle Analyzer. The adsorption of PNP using 0.1 gram of adsorbent using the batch method reached optimum conditions at pH 6 and a contact time of 120 minutes. The PNP adsorption process followed a pseudo-second-order adsorption kinetics model with a maximum adsorption capacity of 3.598 mg/g. These results demonstrate that the developed alginate/PVA/Fe_3O_4 beads exhibit promising potential as a magnetically separable adsorbent for the removal of PNP from aqueous systems

Keywords: *Adsorption; alginate; Fe_3O_4; p-nitrophenol; PVA*

* Corresponding author
Email addresses: sonya@unper.ac.id (SN Vikandari)

DOI: https://doi.org/10.22437/chp.v10i1.50987
Received December 08th 2025; **Accepted** May 17th 2026; **Available online** June 30th 2026
Copyright © 2026 by Authors, Published by Chempublish Journal. This is an open access article under the CC BY License (https://creativecommons.org/licenses/by/4.0)

Graphical Abstract

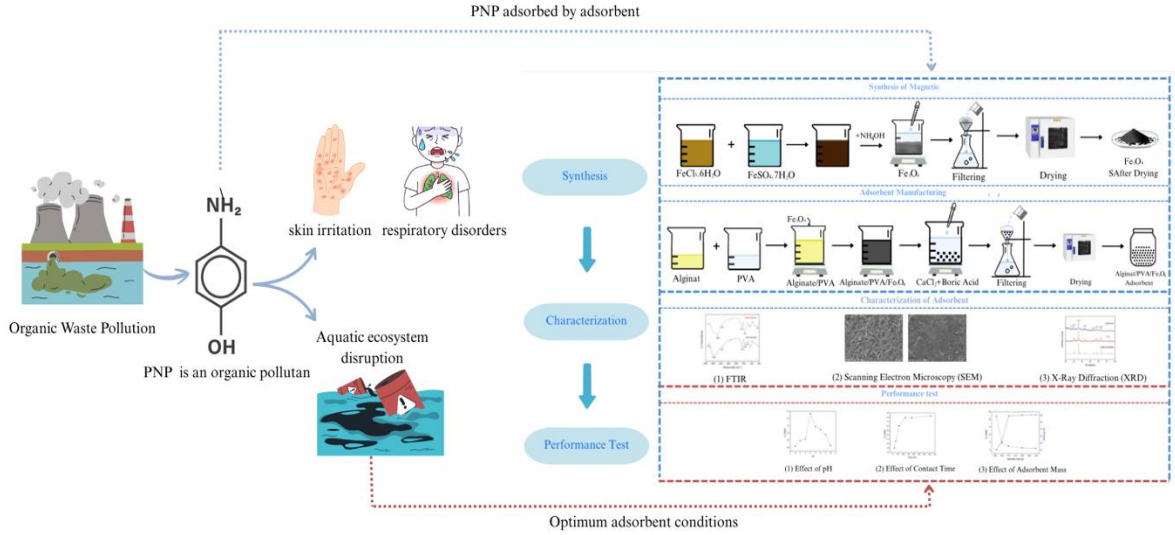

Introduction

P-nitrophenol (PNP) is a priority pollutant with carcinogenic and highly toxic properties, recognized as a priority pollutant by the United States Environmental Protection Agency (US EPA). PNP is used in various industries, including pharmaceuticals, pesticides, and dyes, which frequently discharge waste into aquatic systems, raising concerns of human health and aquatic ecosystems [1]. Long-term exposure to PNP can cause symptoms ranging from skin irritation to more serious health problems such as organ damage, anemia, and respiratory problems [2]. Various methods have been developed to remove PNP, such as photocatalytic degradation [3], oxidation [4], catalytic reduction [5], electrocoagulation [6], and adsorption [7,8]. Among these methods, adsorption is considered the most effective because easy to do, highly efficient, requires a short time, does not produce harmful by-products, environmentally friendly, and can reuse the adsorbent [8,9]. However, the effectiveness of the adsorption process is highly dependen to the selection of the right adsorbent.

Several studies showed the use of adsorbents for the adsorption of PNP from waste. The use of activated tea waste (ATW) as an economical adsorbent because it has the potential to effectively remove PNP through physical interactions including hydrogen bonds between the hydroxyl groups in PNP and the active functional groups in ATW [10]. Mesoporous silica, aminopropyl-modified MCM-48, showed significant adsorption efficiency for various nitrophenolic compounds with optimal performance at a specific pH [11]. Adsorption effectiveness can also be influenced by other inorganic materials, for example aluminum combined with reduced graphene oxide has been shown to increase the removal efficiency of PNP [12]. The use of alginate beads as an adsorbent for nitrophenol adsorption with a removal percentage of 75% at neutral pH [13]. Alginate/Fe_3O_4 magsorbent for nitrophenol removal with a removal percentage of 20% [14].

Alginate biopolymer derived from brown algae can be applied as an adsorbent to adsorb various types of waste. The chemical structure of alginate has carboxyl and

hydroxyl groups that can increase its chelating properties and ionic capacity [15,16]. The use of alginate beads in Rusnadi's research showed that the immobilization process can increase the stability and efficiency of adsorption performance [17]. One of the advantages of alginate is its flexibility to be made in various physical forms including gels, films, or beads [18]. Another advantage is that alginate is a non-toxic and biodegradable biopolymer compared to other synthetic adsorbents [16]. However, alginate has the disadvantage of being rigid and weak, so it needs to be modified using synthetic polymers such as flexible and compatible polyvinyl alcohol [19, 20].

Polyvinyl Alcohol (PVA) is a synthetic polymer that has high solubility, biodegradability, and good chemical stability. In addition, PVA is a preferred matrix because it has a porous structure that allows the substrate to diffuse into the pores [21]. Modified alginate/PVA beads have high strength compared to alginate granules and non-toxic effects when decomposed in water. The application of Alginate/PVA in adsorption PNP has difficulties in the process of transferring or separating the adsorbent after adsorption from the solution, so that magnetic Fe_3O_4 is needed to facilitate the separation of the adsorbent with the help of an external magnetic field after the adsorption process completed [17,22]. Modified alginate/PVA/Fe_3O_4 has a strong double cross-linked structure so it has high magnetic stability.

Although alginate and alginate/Fe_3O_4-based adsorbents have been studied for PNP removal, and alginate/PVA/Fe_3O_4 composites have been reported for other applications, studies specifically investigating the use of alginate/PVA/Fe_3O_4 for PNP adsorption are still limited. Therefore, this study aims to synthesize and characterize alginate/PVA/Fe_3O_4 composite beads and evaluate their performance for PNP removal. The novelty of this study lies in the integration of improved mechanical properties from PVA and magnetic separability from Fe_3O_4 into an alginate-based system, which is expected to enhance adsorption performance

Materials and Methods

Materials

Alginate (Sigma Aldrich), polyvinyl alcohol (PVA), iron (III) chloride hexahydrate ($FeCl_3.6H_2O$), iron (II) sulfate heptahydrate ($FeSO_4.7H_2O$), p-nitrophenol (PNP), ammonium hydroxide (NH_4OH), hydrochloric acid (HCl), sodium hydroxide (NaOH), calcium chloride ($CaCl_2$), boric acid (H_3BO_3), and distilled water.

Fe_3O_4 Synthesis

The Fe^{3+} solution from solid $FeCl_3.6H_2O$ was mixed with the Fe^{2+} solution from solid $FeSO_4.7H_2O$ in a 2:1 ratio until homogeneous. The mixture was slowly added with NH_4OH and stirred using a magnetic stirrer at 300 rpm for 20 minutes at 60°C. NH_4OH is added until the pH of the solution until base condition (pH ±10), which is monitored using a pH meter. The solution was filtered and washed with distilled water. The filtered filtrate was dried with oven at 60°C. The presence of a precipitate indicates the successful formation of magnetic Fe_3O_4. [15,20,21]

Preparation of Alginate/PVA/Fe_3O_4

A 6% alginate solution was prepared by dissolving 6 grams of sodium alginate in 100 mL of distilled water and stirring using a magnetic stirrer until homogeneous. A 3% PVA solution was prepared by dissolving 3 grams of PVA in 100 mL of distilled water.

The two solutions were mixed and stirred until homogeneous. Fe_3O_4 (1% w/v, equivalent to 2 g in 200 mL of the alginate/PVA mixture) was added into the solution and stirred using a stirring rod. The alginate/PVA/Fe_3O_4 mixture was added dropwise to a mixture of 2% $CaCl_2$ and 6% boric acid using a pipette until alginate/PVA/Fe_3O_4 beads were formed. The beads were left in the $CaCl_2$ solution for 24 hours and then washed repeatedly with distilled water. The beads were dried in an oven at 60°C [15,23]

Characterization of Alginate/PVA/Fe_3O_4

This characterization was carried out to compare the condition of the adsorbent before and after use in the adsorption process. The functional groups of the adsorbent were characterized using Fourier Transform Infrared Spectroscopy (FTIR, IR Prestige 21) with KBr pellets at wavenumbers of 4000-450 cm^{-1}. The surface morphology of the adsorbent was characterized using Scanning Electron Microscopy (SEM, SEM SU3500). The crystal structure of the adsorbent was characterized using X-ray Diffraction (XRD, Bruker D8 Advance X-Ray Diffractometer), and the adsorbent charge at several pH values was analyzed using Zeta Potential (Horiba SZ-100 Nano Particle Analyzer).

Batch Method

The adsorption experiments were conducted using a batch method. A specific volume and concentration of adsorbent were added to a PNP solution, then the mixture was stirred using shaker at 120 rpm at room temperature. The effect of pH (3–10) was studied using 20 mL of 20 ppm PNP concentration and 0.1 gram of adsorbent. The pH of the solution was adjusted using 0.1 M HCl or 0.1 M NaOH. The effect of contact time (15–360 minutes) was studied using 20 mL of 20 ppm PNP concentration and 0.1 gram of adsorbent at optimum pH conditions. The effect of adsorbent mass (0.01–0.3 grams) was studied at the optimum pH and contact time conditions. After the adsorption process, the adsorbent was separated using an external magnet, and the PNP concentration was analyzed using a UV-Vis. Each experiment was performed in triplicate for all parameters.

Calculation of adsorption capacity and adsorption percentage as equation 1 and 2.

$$q_e = \frac{(C_i - C_e)\,V}{m} \quad (1)$$

$$\text{Removal}\ (\%) = \frac{(C_i - C_e)}{C_i}\ x\ 100 \quad (2)$$

where q_e is the adsorption capacity (mg/g), C_i is the initial concentration of PNP (mg/L), C_e is the equilibrium concentration (mg/L), V is the solution volume (L), and m is the mass of the adsorbent (g).

Results and Discussions

FTIR Analysis

The FTIR spectra of the adsorbent before and after adsorption can be seen in Figure 1. This shift occurs in the O–H band from 3220 to 3449 cm^{-1}, indicating the involvement of hydroxyl groups in hydrogen bonding interactions with PNP molecules. These results indicate that hydrogen bonding interactions are one of the mechanisms that occur between the hydroxyl groups in the alginate/PVA adsorbent matrix and the phenolic –OH groups of PNP. The shift in asymmetric and symmetric COO^- bands from 1612 to 1602 cm^{-1} and 1431 to 1423 cm^{-1}, indicates the presence of carboxylic groups in electrostatic interactions. At the working pH (see the discussion of optimum pH), PNP is present in its phenolic form, which can

interact electrostatically with positively charged sites on the adsorbent surface or form ion-dipole interactions with COO^- groups. the formation of hydrogen bonds and electrostatic interactions between the adsorbent and PNP. A new band at 1272 cm^{-1} indicates the presence of C–O stretching of the phenolic group or NO_2 related vibrations that confirm the successful attachment of PNP to the adsorbent surface, the presence of PNP on the adsorbent. In addition, the Fe–O band at wave number 555 cm^{-1} appears unclear after the adsorption process because the Fe_3O_4 site is partially covered by PNP molecules as evidenced by SEM observations, the surface morphology becomes rough and more closed after adsorption.

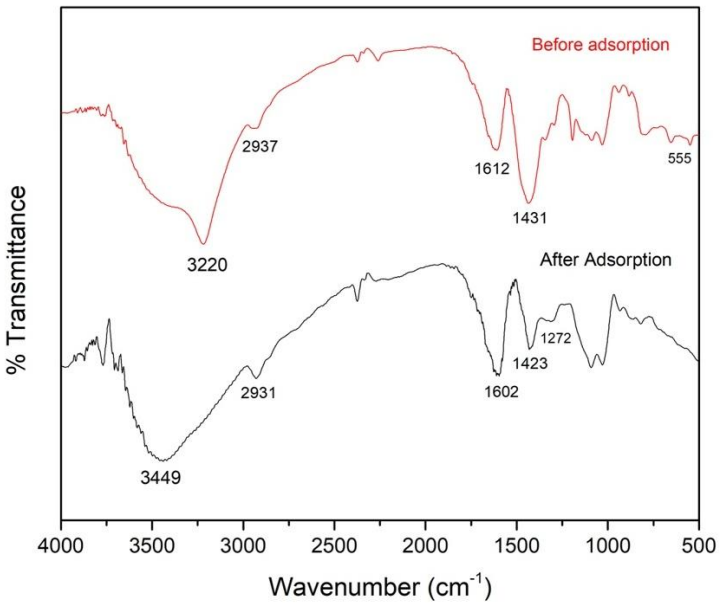

Figure 1. FTIR Spectrum of adsorbent before and after p-nitrophenol adsorption

SEM Analysis

The surface morphology of the adsorbent before and after the adsorption process is shown in Figure 2. The surface of the alginate/PVA/Fe_3O_4 adsorbent before adsorption is relatively inhomogeneous, rough and porous surface. This indicates the potential for active sites on the adsorbent to interact with the adsorbate [24]. The porous structure plays a role in facilitating the diffusion of the adsorbate into the adsorbent matrix and increasing the intensity of interactions with surface functional groups. Meanwhile, the SEM image of the alginate/PVA/Fe_3O_4 adsorbent after the adsorption process has a smooth surface, indicating that the adsorbate has filled and covered the pores in the adsorbent [23]. Thus, the adsorption process occurs on the surface of the adsorbent pores, characterized by the formation of an adsorbate layer on the adsorbent surface [25].

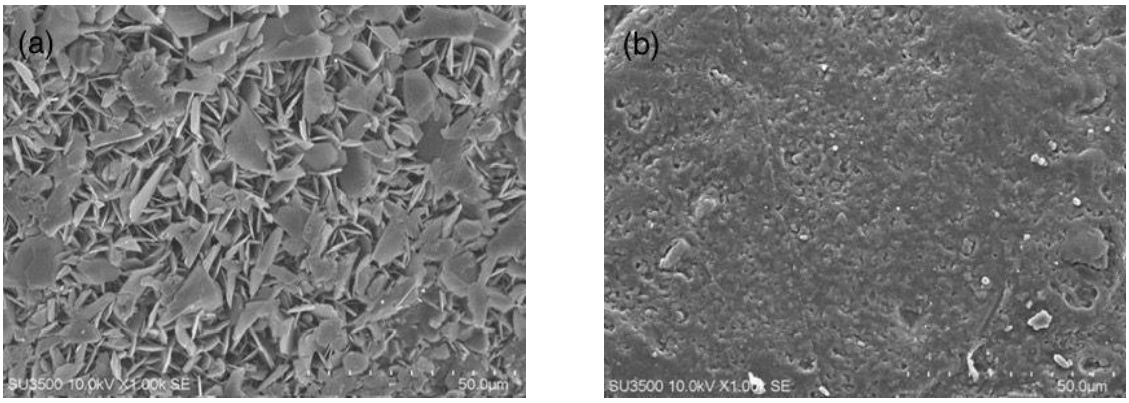

Figure 2. SEM image of Alginate/PVA/Fe_3O_4 adsorbent (a) before p-nitrophenol adsorption, (b) after p-nitrophenol adsorption

XRD Analysis

The crystal structure and presence of magnetite Fe_3O_4 in the adsorbent can be seen in Figure 3. The XRD characterization results show no significant shift in the main peak of Fe_3O_4. The diffractogram shows the main peak at 2θ around 30.1°; 35.5°; 43.2°; 53.6°; 57.1°; and 62.7°. The peak positions produced in the X-ray diffraction (XRD) analysis of the sample show agreement with the standard pattern of the Joint Committee on Powder Diffraction Standards (JCPDS) No. 19-0629, thus confirming that the magnetite phase (Fe_3O_4) was successfully formed in the adsorbent [26]. The Diffraction peaks indicate that Fe_3O_4 has good crystalline properties in the adsorbent matrix [27]. This crystallinity indicates a stable atomic structure order, thus Fe_3O_4 plays a role in providing structural stability to the alginate/PVA/Fe_3O_4 composite. In addition, the presence of the crystalline Fe_3O_4 phase also has the potential to provide active sites in the adsorption process [28].

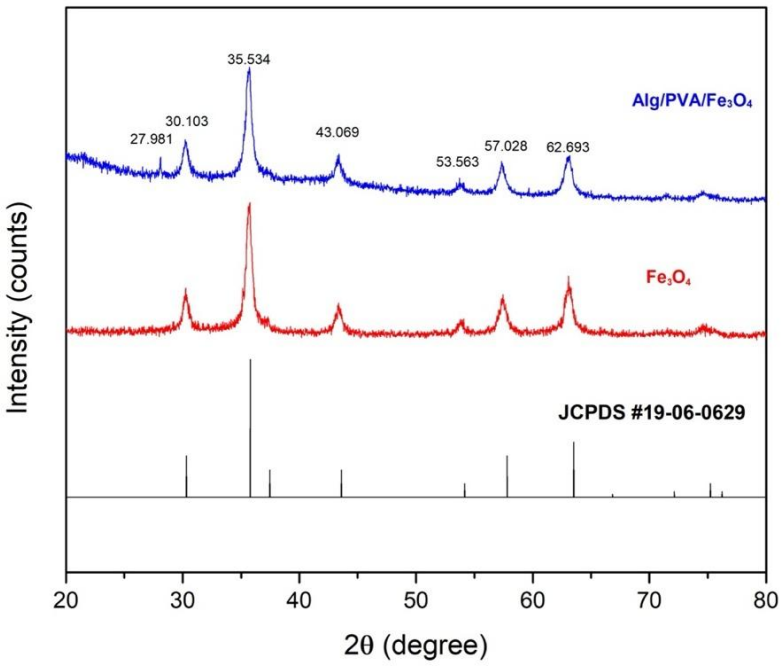

Figure 3. XRD patterns of Alginate/PVA/Fe_3O_4 adsorbent, pure Fe_3O_4, and the standart Fe_3O_4 diffraction pattern from the JCPDS database

Effect of pH

pH optimization was performed in the pH range of 3-10 using HCl and NaOH solutions. The pH optimization was performed under conditions of 20 mg/L PNP for a contact time of 60 minutes, an adsorbent mass of 0.1 gram, and a stirring speed of 150 rpm, as shown in Figure 4. pH 6 is the optimum condition for the PNP adsorption process. The zeta potential measurement of alginate/PVA/Fe_3O_4 adsorbent at pH 4 had a value of -3.3 mV, pH 6 had a value of -3.7 mV and pH 9 had a value of -11.3 mV. This shows that increasing pH (increasingly base conditions) causes the surface of the adsorbent to be increasingly negatively charged. At pH 6, the negative charge on the adsorbent surface is relatively low, while phenol does not dissociate, resulting in a balance between hydrogen bonding and electrostatic interactions. Adsorption capacity increases at pH 3 to 6 because the adsorbent surface has a nearly neutral charge, allowing it to interact with the negatively charged PNP. At acidic pH, the removal percentage is higher because phenol does not dissociate, and dispersion interactions are more dominant. PNP has a pKa of 7.15, indicating that PNP contains phenolate ions that are negatively charged when they exceed the pKa value [7]. So that in base conditions, there is a repulsive force between the adsorbent and PNP, which can reduce the adsorption capacity [29]. The results are in agreement with previous reports on the adsorption PNP using alginate, that electrostatic interaction between $–COO^-$ groups of alginate and protonated species of PNP plays an important role in the adsorption process [13,30]

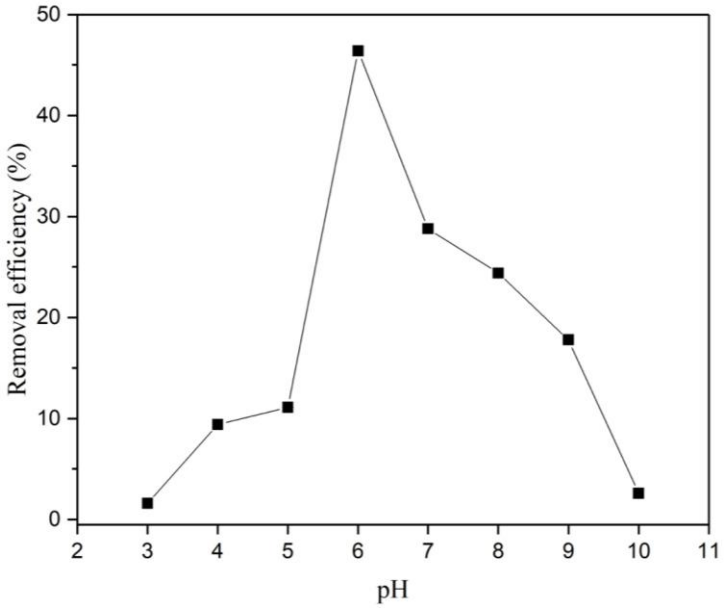

Figure 4. Effect of pH on the removal efficiency of p-nitrophenol using Alginate/PVA/Fe_3O_4 adsorbent.

Effect of Contact Time

Contact time optimization was performed at various time intervals (15–360 minutes) with an adsorbent mass of 0.1 gram and a PNP solution of 20 mg/L at pH 6, as shown in Figure 5. The optimum contact time was 120 minutes. The amount of PNP adsorbed increased gradually until equilibrium was reached. This is because the longer the adsorption time, the more active sites on the adsorbent surface will be increased,

resulting in more adsorbate being adsorbed [31]. However, the adsorption capacity remains constant after reaching equilibrium because the active sites of the adsorbent have completely interacted with the adsorbate. Once the equilibrium condition is reached, this time is used as a reference for the contact time in the next experiment [32]

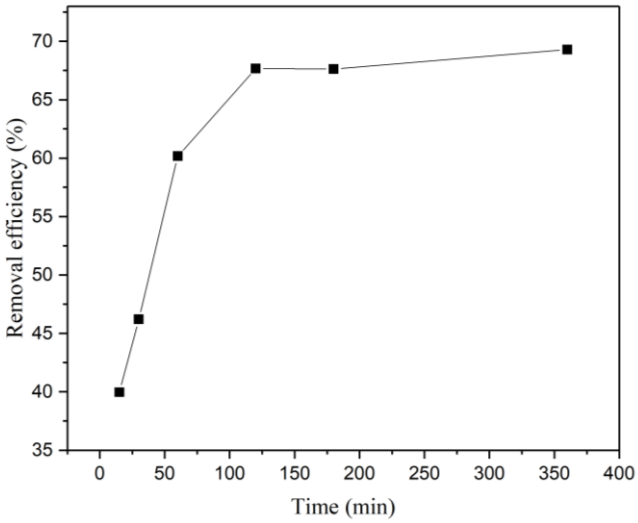

Figure 5. Effect of Contact Time on the removal efficiency of p-nitrophenol using Alginate/PVA/Fe_3O_4 adsorbent

Effect of Adsorben Mass

The conditions for adsorbent mass were a 25 mL volume of 20 ppm PNP solution at pH 6 and a contact time of 120 minutes. The mass variation used ranged from 0.05 to 0.3 grams. Based on Figure 6, the optimal adsorbent mass obtained was 0.1 gram and was constant at the following adsorbent mass. The influence of adsorbent mass can decrease the adsorption capacity and increase the adsorption percentage. As the adsorbent mass increases, the number of active sites increases. Otherwise, a disproportion between the overbalance amount of adsorbent and the PNP concentration in the solution will reduce the adsorption capacity [33]

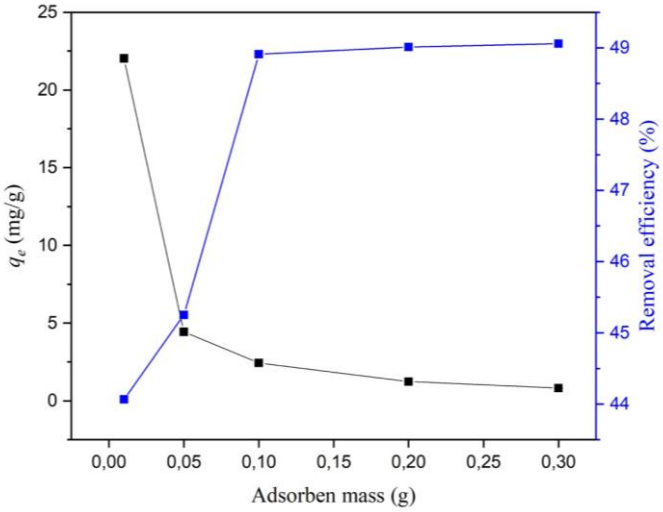

Figure 6. Effect of Adsorbent Mass on adsorption capacity and percentage removal of p-nitrophenol using Alginate/PVA/Fe_3O_4.

Kinetics Adsorption

The adsorption mechanisms used in this study were pseudo-first-order and pseudo-second-order kinetic models. The PNP concentration used was 20 ppm with an equilibrium contact time of 120 min. The linearized form of the pseudo-first-order kinetic model is expressed in Equation (3) meanwhile, the linearized pseudo-second-order kinetic model is described by Equation (4).

$$\log(q_e - q_t) = \log q_e - \frac{k_1 t}{2{,}302} \quad (3)$$

$$\frac{t}{qt} = \frac{1}{k^2 q_e^2} + \frac{t}{q_e} \quad (4)$$

Where q_t is s the amount of PNP adsorbed by at time (min), q_e is the amount of PNP adsorbed by adsorbent at equilibrium conditions (mg/g), k_1 is equilibrum rate constant of pseudo-first-oder (min^{-1}) and k_2 is the equilibrum rate constant of pseudo-second-order (g/mg.min). These constants are obtained from the experimental data plots of log (q_e-q_t) vs t and (t/q_t) vs t.

Table 1. PNP adsorption kinetic parameters

Model	R^2	q_e theoretical (mg/g)	k_1 (1/min)	k_2 (g/mg.min)	q_e experimental (mg/g)
Pseudo-first-order	0.0185	0.7383	0.00138	-	
Pseudo-second-order	0.995	3.598	-	0.2631	3.46499

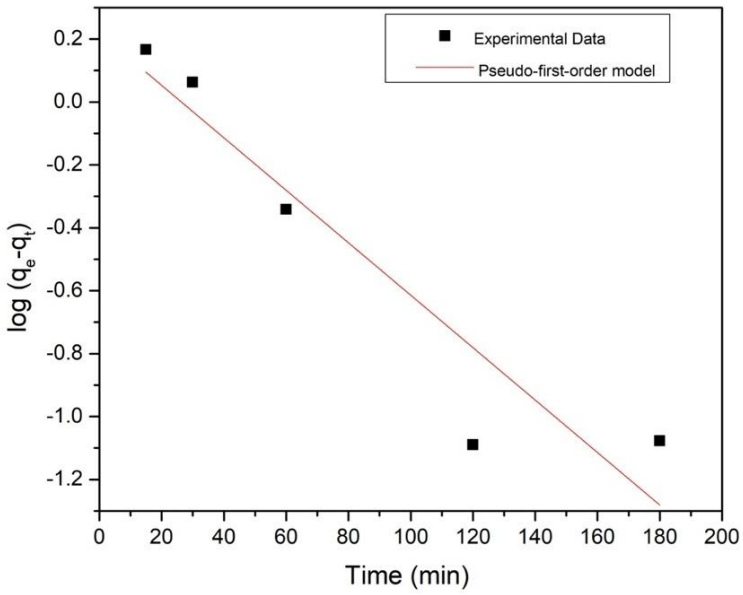

Figure 7. Fitting linear pseudo-first order for p-nitrophenol adsorption onto Alginate/PVA/Fe_3O_4

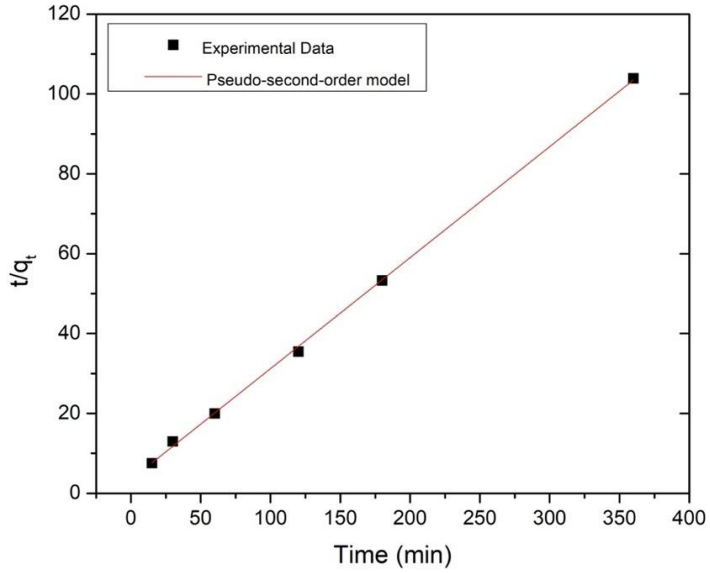

Figure 8. Fitting linear pseudo-second order for p-nitrophenol adsorption onto Alginate/PVA/Fe_3O_4.

Based on Table 1, The pseudo-second-order kinetic model exhibits a significantly higher correlation coefficient (R^2 = 0.995) than the pseudo-first-order model (R^2 = 0.0185). In addition, the calculated adsorption capacity (3.598 mg/g) is in close agreement with the experimental value (3.46499 mg/g), indicating that the adsorption of PNP onto alginate/PVA/Fe_3O_4 is better described by the pseudo-second-order. The pseudo-first-order model is generally associated with physisorption, while the pseudo-second-order model is related to chemisorption. In this study, both models showed comparable R^2 values, indicating that the adsorption of PNPs on alginate/PVA/Fe_3O_4 involves weak physical interactions and stronger chemical bonds [34]. The analysis of adsorption kinetics suggests that the process is primarily controlled by chemisorption occurring at heterogeneous active sites on the adsorbent surface. which involves the sharing or exchange of electrons between the active sites of the alginate/PVA/Fe_3O_4 adsorbent and PNP molecules in solution. The results in line with previous kinetic studies on the adsorption of various dyes using calcium alginate/activated carbon composite beads [35]. To further evaluate the adsorption performance of the prepared adsorbent, a comparison with previously reported adsorbents for PNP removal was conducted.

Tabel 2. Comparison of the adsorption of PNP with other reported adsorbents

Adsorbents	Optimum condition	Adsorbent capacity	Kinetic model	References
Alginate beads	pH = 7; t=12 h; m= 0,22g	0.69 mg/g	-	[13]
Nanographite Oxide	pH = 7; t=2 h; m = 1 g	268.5 mg/g	PSO	[7]
Activated Carbon	-	340; 350; and 365 mg/g (with different size)	PFO & PSO	[36]
Pili Nut Shell Activated Carbon.	pH=6; t = 60 min; m = 0,03 g;	190.39 mg/g	PSO	[37]

Adsorbents	Optimum condition	Adsorbent capacity	Kinetic model	References
Activated Carbon produced from Alhagi	pH = 8; t=150 min	17.254 mg/g	PSO	[38]
Alg/PVA/Fe_3O_4 beads	pH = 6; t = 120 min; m = 0.05 g	3.598 mg/g	PSO	This work

Table 2 presents the adsorption performance of various adsorbents for PNP removal reported in previous studies and this work. It can be observed that the adsorption capacity of Alg/PVA/Fe_3O_4 beads (3.598 mg/g) is lower than some reported adsorbents such as activated carbon and nanographite oxide. However, the adsorption process follows a pseudo-second-order kinetic model, indicating that the adsorption mechanism is chemisorption. In addition, the obtained performance was achieved indicates that the prepared adsorbent remains a promising alternative material for PNP removal. Furthermore, the presence of Fe_3O_4 offers advantages in terms of magnetic separation in facilitating the separation of the adsorbent from the adsorbate.

Conclusions

The alginate/PVA/Fe_3O_4 adsorbent was successfully synthesized and characterized using FTIR spectrophotometer, SEM, XRD, and Zeta potential. The alginate/PVA/Fe_3O_4 adsorbent successfully adsorbed PNP using the batch method under optimum conditions at pH 6, contact time 120 minutes, and a PNP solution volume of 25 mL. The adsorption process followed a pseudo-second-order kinetic model with a maximum adsorption capacity of 3.598 mg/g.

Acknowledgement

This research is supported by the Ministry of Higher Education, Science, and Technology through the 2025 Kemdiktisaintek Grant Programme for the financial support provided to enable this research to be successfully conducted. We also express gratitude to the Perjuangan University of Tasikmalaya and the Bandung Institute of Technology for the facilities provide during the research program.

Author Contributions

Conceptualization, Methodology, SNV; Validation, Formal Analysisis, SNV. and FAF; Investigation, SNV., FAF., NS., NRA.; Resources, SNV.; Data Curation, SNV. and FAF.; Writing, original draft preparation, SNV.; Writing, review & Editing, SNV and FAF. All authors have read and agreed to the published version of the manuscript

Conflict of Interest

The authors declare no conflict of interest.

References

[1] Racles, C., Zaltariov M. F., Damoc M., Macsim A. M., Iacob, M., Sacarescu, L Three Reactions, One Catalyst: A multi-Purpose platinum(IV) complex and its silica-supported homologue for environmentally friendly processes. *Applied Organometallic Chemistry*. 2020, 34(3). DOI: 10.1002/aoc.5422

[2] Pourkhanali, K., Saleh, M., Khayati, G. Performance evaluation of bulk liquid membrane technique on p-nitrophenol removal from aqueous solution. *Chemical and Biochemical Engineering Quarterly*. 2018, 32 (1), 83–90. DOI:10.15255/CABEQ.2016.1033.

[3] Velusamy, S., Roy, A., Mariam, E., Krishnamurthy, S., Sundaram, S., Mallick, T. K. Effectual visible light photocatalytic reduction of para-nitro phenol using reduced graphene oxide and ZnO composite. *Scientific Report.* 2023, 13, 2260-2269. DOI: 10.1038/s41598-023-36574-7

[4] Lin, X. Q., Kong, W. M., Lin, X. Degradation of high-concentration p-nitrophenol by Fenton oxidation. *Water Science and Technology.* 2020, 81, 2260–2269. DOI: 10.2166/wst.2020.284

[5] Kassem, A. A., Abdelhamid, H. N., Fouad, D. M., Ibrahim, S. A. Catalytic reduction of 4-nitrophenol using copper terephthalate frameworks and CuO@C composite. *Journal of Environmental Chemical Engineer.* 2021, 9(1), 2213-3437. DOI: 10.1016/j.jece.2020.104401

[6] Modirshahla, N., Behnajady, M. A., Mohammadi, A. S. Investigation of the effect of different electrodes and their connections on the removal efficiency of 4-nitrophenol from aqueous solution by electrocoagulation. *Journal of Hazardous Materials*. 2008, 154(1), 778–786. DOI: 10.1016/j.jhazmat.2007.10.120.

[7] Zhang, B., Li, F., Wu, T., Sun, D., Li, Y. Adsorption of p-nitrophenol from aqueous solutions using nanographite oxide. *Colloids and Surfaces A: Physicochemical and Engineering Aspects.* 2015, 464, 78–88. DOI: 10.1016/j.colsurfa.2014.10.020.

[8] Cheng, M., Jiang, J., Wang, J., Fan, J., Highly Salt Resistant Polymer Supported Ionic Liquid Adsorbent for Ultrahigh Capacity Removal of p-Nitrophenol from Water. *ACS Sustainable Chemistry and Engineering*. 2019, 9(7). DOI: 10.1021/acssuschemeng.8b06198.

[9] Zango, Z. U., Sambudi, N. S., Jumbri, K., Ramli, A., Bakar, N., Saad, B., Roizaini, M., Isiyaka, H., Osman, A., Sulieman, A. An overview and evaluation of highly porous adsorbent materials for polycyclic aromatic hydrocarbons and phenols removal from wastewater. *Water*. 2020, 12 (10), 1–40. DOI: 10.3390/w12102921

[10] Ahmaruzzaman, M., Gayatri, S. L. Activated tea waste as a potential low-cost adsorbent for the removal of p - nitrophenol from wastewater. *Journal of Chemical and Engineering Data*. 2010, 55 (11), 4614–23. DOI: 10.1021/je100117s.

[11] Gu, X., Kang, H., Li, H., Liu, X., Dong, F., Fu, M., Chen, J. Adsorption removal of various nitrophenols in aqueous solution by aminopropyl-modified mesoporous MCM-48. *Journal of Chemical and Engineering Data.* 2018, 63(9), 3606–3614. DOI: 10.1021/acs.jced.8b00477.

[12] Wu, Z., Yuan, X., Zhong, H., Wang, H., Zeng, G., Chen, X., Wang, H., Zhang, L., Shao, J. Enhanced adsorptive removal of p-nitrophenol from water by aluminum metal-organic. *Scientific Reports*. 2016, 6, DOI: 10.1038/srep25638.

[13] Peretz, S., Cinteza, O. Removal of some nitrophenol contaminants using alginate gel beads. *Colloids and Surfaces A Physicochemical and Engineering Aspect*. 2008, 319, 165–72. DOI: 10.1016/j.colsurfa.2007.06.012.

[14] Obeid, L., Kolli, N., Talbot, D., Welschbillig, M., Bée, A. Influence of a cationic surfactant on adsorption of p-nitrophenol by a magsorbent based on magnetic alginate beads. *Journal of Colloid and Interface Science*. 2015, 457, 218–24. DOI: 10.1016/j.jcis.2015.07.017.

[15] Te, C. L., Manap, N., Zuhudi, A.H., Izwana, I.M. Polyvinyl Alcohol-Alginate Adsorbent Beads for Chromium (VI) Removal. *International Journal of Engineering & Technology.* 2018, 7, 95–99. DOI: 10.14419/ijet.v7i3.20.18988.

[16] Cheng, Y., Lin, H. Y., Chen, Z., Megharaj, M., Naidu, R. Biodegradation of crystal violet using Burkholderia vietnamiensis C09V immobilized on PVA-sodium alginate-kaolin gel beads. *Ecotoxicology and Environmental Safety*. 2012, 83, 108–114. DOI: 10.1016/j.ecoenv.2012.06.017.

[17] Rusnadi, R. Safitri, I. Pembuatan dan Penggunaan Bulir Kalsium Alginat-PVA (Polivinil Alkohol) untuk Adsorpsi Ion Cd(II). *Jurnal Kartika Kimia*. 2023, 6(1), 38-44. DOI: 10.26874/jkk.v6i1.200.

[18] Asif, M., Ullah, S., Khan, A. S., Nasrullah, A., Khitab, F., Ullah, W., Khan, S., Shah, M., Fagieh, T., Ahmed, N. PVA-Alginate beads loaded with activated carbon, Fe_3O_4 nanoparticles and ionic liquids for methylene blue adsorption and their comparison with membrane 2024. *Research Square.* 2024. DOI: 21203/rs.3.rs-4968384/v1.

[19] Deng, S., Huang, X., Kang, Z., Xu, D., Luo, W., Li, D. Penggunaan bahan elektrospinning polivinil alkohol untuk pembalut luka kulit. Journal of Materials Science: Material in Medicine. 2025. 36(1):84. doi: 10.1007/s10856-025-06945-9.

[20] Rahmayanti, M. Sintesis dan karakterisasi magnetit (Fe_3O_4): studi komparasi metode konvensional dan metode sonokimia. *Al Ulum Sains dan Teknologi.* 2020, 6(1), 26-31

[21] Taib, S., Suharyadi, D.E. Sintesis Nanopartikel Magnetite (Fe_3O_4) dengan template silika (SiO_2) dan Karakterisasi Sifat Kemagnetannya. *Indonesian Journal of Applied Physics.* 2015, 5(1), 23-30

[22] Younas, F., Mustafa, A., Farooqi, Z. U. R., Wang, X., Younas, S., Mohy-Ud-din, W., Hameed, M., Abrar, M., Maitlo, A., Noreen, S., Hussain, M. Current and emerging adsorbent technologies for wastewater treatment: Trends, limitations, and environmental implications. *Water* (Switzerland). 2021, 13(2), 1-25. DOI: 10.3390/w13020215.

[23] Li, J., Hu, Z., Chen, Y., Deng, R. Removal of Pb(II) by adsorption of HCO–(Fe_3O_4) Composite Adsorbent: Efficacy and Mechanism. *Water (Switzerland)*, 2023, 15(10), 1-17. doi: 10.3390/w15101857.

[24] Bih, N. L., Rwiza, M. J., Ripanda, A. S., Mahamat, A. A., Machunda, R.L., Choi, J. W. Adsorption of phenol and methylene blue contaminants onto high-performance catalytic activated carbon from biomass residues. Heliyon. 2025, 11(1), DOI: 10.1016/j.heliyon.2024.e41150.

[25] Almas, M., Khan, A. S., Nasrullah, A., Din, I. U., Fagieh, T. M., Bakhsh, E. M., Akhtar, K., Khan, S., Khan, S., Inayat, A. Substantial increase in adsorption efficiency of local clay-alginate beads toward methylene blue impregnated with SDS. *Environmental Science and Pollution Research*. 2023, 30(34), 81433-81449. DOI: 10.1007/s11356-022-23949-y.

[26] Cassia, M. D., Sugihartono, I., Purwandanu, S. H., Futukhillah, F. A. A., Triyono, D., Setiawan, M. R, Swee, T. T. Synthesis and characterization analysis of Fe_3O_4 /SiO_2 core shelL. SPEKTRA: *Jurnal Fisika dan Aplikasinya*. 2023, 8(3), 161-167, DOI: 10.21009/SPEKTRA.

[27] Rahadianto, W. T., Sugesti, H., Chandra, Y. Equilibrium journal of chemical engineering Synthesis and Application of Coconut Shell Activated Carbon Fe_3O_4 Composite for Zn^{2+} Metal Ion Adsorption from Wastewater. Equilibrium Journal of Chemical Engineering. 2025, 9(2), 54-59. DOI: 10.20961/equilibrium.v9i2.11178.

[28] Panda, S. K., Aggarwal, I., Kumar, H., Prasad, L., Kumar, A., Sharma, A., VO, D., Van, T. D., Mishra, V. Magnetite nanoparticles as sorbents for dye removal: a review. Environmental Chemistry Letters. 2021, 19(2), 2487–5225. DOI: 10.1007/s10311-020-01173-9.

[29] Ma, H., Xu, Z., Wang, W., Gao, X., Ma, H. Adsorption and regeneration of leaf-based biochar for: P -nitrophenol adsorption from aqueous solution. *RSC Advances*. 2019, 9(67), 39282–39293. DOI: 10.1039/c9ra07943b.

[30] Ashrafi, S. D., Safari, G. H., Sharafi, K., Kamani, H., Jaafari, J. Adsorption of 4-Nitrophenol on calcium alginate-multiwall carbon nanotube beads: Modeling, kinetics, equilibriums and reusability studies. *International Journal of Biological Macromolecules*. 2021, 185, 66–76. DOI: 10.1016/j.ijbiomac.2021.06.081.

[31] Fahri, H., Zulfikar, M. A., Azis, M. Y. Synthesis of Molecularly Imprinted Polymers with Magnetite Cores for Ibuprofen Adsorption. *Jurnal Kimia Sains dan Aplikasi*. 2024, 27(1), 28–34. DOI: 10.14710/jksa.27.1.28-34.

[32] Tran, H. N., Wang, Y. F., You, S. J., Chao, H.P. Insights into the mechanism of cationic dye adsorption on activated charcoal: The importance of Π–Π interactions. *Process Safety and*

Environmental Protection. 2017, 107, 168–80. DOI: 10.1016/j.psep.2017.02.010.

[33] Algethami, J. S., Alqadami, A. A., Melhi, S., Alhamami, M. A. M., Fallatah, A. M., Rizk, M. A. Sulfhydryl Functionalized Magnetic Chitosan as an Efficient Adsorbent for High-Performance Removal of Cd(II) from Water: Adsorption Isotherms, Kinetic, and Reusability Studies. *Adsorption Science and Technology.* 2022, 1-16. doi: 10.1155/2022/2248249.

[34] Dimbo, D., Abewaa, M., Adino, E., Mengistu, A., Takele, T., Oro, A., Rangaraju, M. Methylene blue adsorption from aqueous solution using activated carbon of spathodea campanulata. *Results in Engineering.* 2024, 21. DOI: 10.1016/j.rineng.2024.101910.

[35] Song, Y., Wang, S., Yang, L. Y., Yu, D., Wang, Y. G., Ouyang, X. Facile fabrication of core–shell/bead-like ethylenediamine-functionalized Al-pillared montmorillonite/calcium alginate for As(V) ion adsorption. *International Journal of Bioligical Macromolecules*. 2019, 131, 971–979. DOI: 10.1016/j.ijbiomac.2019.03.172.

[36] Ledesma, B., Sabio, E., González-García, C. M., Román, S., Fernandez, M. E. , Bonelli P., Cukierman, A. Batch and Continuous Column Adsorption of p-Nitrophenol onto Activated Carbons with Different Particle Sizes. Processes. 2023, 11(7), DOI: 10.3390/pr11072045.

[37] Nwosu, F. O. Adekola, F. A., Salami, A. O. Adsorption of 4-Nitrophenol (PNP) Using Pilli Nut Shell Active Carbon. Pakistan *Journal of Analytical & Environmental Chemistry.* 2017, 18 (1), 69–83. DOI: 10.21743/pjaec/2017.06.07.

[38] Abd-Hadi, G. M., Salman, S. D. Adsorption of para nitro-phenol by activated carbon produced from alhagi. *Sains Malaysiana*. 2020, 49(1), 57–67. DOI: 10.17576/jsm-2020-4901-07.